High Resolution Molecular Spectroscopy of Methanol Isotopes in the Far-Infrared

John Sullivan
Heidi Hockel
Michael Lauters

Faculty Sponsors: Gubbi Sudhakaran and Michael Jackson
Department of Physics

ABSTRACT

Several techniques have been used to investigate the methanol isotopes $^{13}CH_3OH$, CD_3OH, CD_3OD, $^{13}CD_3OD$ and CHD_2OH in the far-infrared (FIR) region. In the first experiment, a carbon dioxide laser was used to optically pump a FIR laser cavity containing the methanol isotope. The FIR laser utilized an X-V pumping geometry, recently shown to efficiently pump short wavelength emissions below 100 μm. With this pumping geometry, over forty new laser emissions have been discovered, eighteen of which are reported in this work. Next, the frequencies of these emissions were measured using the three-laser heterodyne technique. In all, the frequencies of forty-three distinct laser emissions, ranging from 44 to 238 μm, have been measured and are reported with a fractional uncertainty up to $\pm 2 \times 10^{-7}$. In addition, the spectroscopic assignment of two laser schemes has been completed and is presented. Finally, a deuterium cyanide laser, operating at 195 μm, has been used to record the Stark spectra of CD_3OD in both parallel and perpendicular polarizations with electric fields up to 60 000 V/cm. One family of resonances has been identified as belonging to the $J_K = 15_2 \leftarrow 16_3\ A^-$, $\upsilon_t = 2$ transition. The Stark voltages and zero-field frequency for this transition are reported.

INTRODUCTION

The most important scientific tool used to decipher the structure of matter has been atomic and molecular spectroscopy. So far, microwave spectroscopy has provided the most precise information available about molecular structures and electric dipole moments. To extend the available information obtained from microwave techniques to higher rotation, torsion-rotation, and/or vibration-rotation energies, studies must be conducted in the FIR region. For the purpose of this work, "far-infrared" spans the wavelength region from 25 μm to 2 mm. Historically, this region has suffered from the lack of sensitive detectors and powerful sources. This situation has changed drastically with the development of nonlinear (point contact diodes) and liquid helium cooled detectors as well as the invention of the direct discharge, optically pumped and tunable FIR lasers.

One of the molecular species having a very rich absorption spectrum in this region is methanol, the simplest asymmetric-top molecule found to exhibit hindered internal rotation. Since the pioneering works of Borden and Dennison [1, 2] numerous studies on methanol and its isotopic species in the infrared, far-infrared and microwave regions have been per-

formed. Recently, detailed global modeling has successfully treated the data from these studies as well as the extensive far-infrared information available from Fourier transform spectroscopy to generate the best-known molecular parameters for methanol [3]. The known theoretical and experimental work have now been collected in a CRC Methanol Atlas, which compiles the spectroscopic results from 0 to 1258 cm^{-1} [4]. Unfortunately there is not a corresponding wealth of data in the literature on several isotopic species of methanol. As a result, the molecular parameters of many isotopic species are known to limited precision and are of marginal use in predicting unobserved lines.

Methanol and its isotopes are also of interest to astrophysicists. Since the discovery of interstellar methanol in 1970 [5], over 200 interstellar lines belonging to methanol have been detected as well as the discovery of interstellar maser emissions [4, 6, 7]. This molecular species has been found to play a significant role in the millimeter- and submillimeter-wave spectra of molecular clouds, particularly in regions of star-formation [8-10]. The correct interpretation and evaluation of this information requires detailed knowledge of the energy levels and transition probabilities of methanol and its isotopes over wide ranges of the spectrum. Finally, the same complexity that makes methanol a nontrivial spectroscopic object also makes it such a prolific FIR laser source. Methanol and its isotopes have been proved to be among the richest and most efficient active molecular laser media known, with over two thousand optically pumped laser lines observed in the FIR region [11-14].

In this paper, we discuss the discovery of new optically pumped laser emissions and the measurement of OPML frequencies from $^{13}CH_3OH$, CD_3OH, CD_3OD, $^{13}CD_3OD$ and CHD_2OH. Also presented are the spectroscopic assignments of several FIR laser schemes for optically pumped $^{13}CH_3OH$ as well as the assignment of the CD_3OD absorption spectra investigated with a direct discharge laser and the Stark effect.

METHOD

The optically pumped molecular laser system consists of a carbon dioxide (CO_2) pump laser and a FIR laser cavity. The CO_2 laser, shown in Fig. 1, is 1.5 m long and includes a partially ribbed cavity surrounded by a water-cooled jacket. The pumping mechanism is in the form of a 15 000 V power supply capable of providing 50 mA to each cathode. The laser medium is a flowing gas mixture of CO_2, Nitrogen and Helium in the ratio 1:1.2:7.8 with

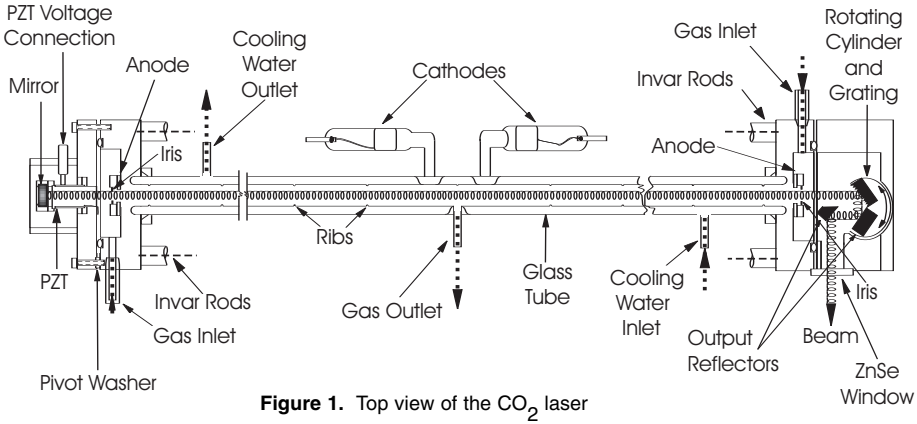

Figure 1. Top view of the CO_2 laser

CO_2 producing the laser emissions while Helium and Nitrogen act as buffer gases. The Pyrex glass tube has an inner diameter of 18 mm and contains five equally spaced glass ribs whose inner diameters increase from 16.5 to 17.5 mm. By introducing glass ribs into the laser cavity many wall bounce modes are eliminated thereby forcing an open structure mode and increasing the effective resolution of the grating [15]. The laser uses the zeroth-order output coupling from a 133 line/millimeter grating with 3% output coupling in zero order. A high-reflectivity gold-coated 20 m radius-of-curvature mirror, attached to a piezo-electric transducer (PZT), is used on the other end. The PZT permits the fine adjustment of the end mirror, allowing the CO_2 laser radiation to be kept tuned to its center frequency. The CO_2 laser is capable of producing approximately 275 lines, including regular, hot, and sequence band emissions. Both the 9 and 10 μm branches exhibit high-J lines out to 9*R*58, 9*P*60, 10*R*58 and 10*P*60. Regular laser lines reach powers up to 30 W with the hot- and sequence-band emissions reaching 10 W [16-18].

The second component of the OPML system is shown in Fig. 2. The CO_2 laser radiation is focused into the FIR cavity with a 12 m radius-of-curvature gold coated concave mirror, externally mounted on the far (fixed mirror) end of the cavity at approximately 2 m from the 20 mm diameter ZnSe window. A flat gold coated mirror then reflects the CO_2 beam into the FIR cavity and to the X-V mirror system. This mirror system, shown in Fig. 2, uses three 19-mm diameter copper mirrors, a gold-coated copper mirror with a 1 m radius of curvature and one of the FIR cavity mirrors. Each of the four copper mirrors extend about 20 mm into the FIR cavity, transmitting approximately 99% of the 118.8 μm line of CH_3OH[1] through the FIR window. The advantage to this is that many of the longer wavelength lines are suppressed, thereby allowing some of the shorter wavelengths to emerge [19].

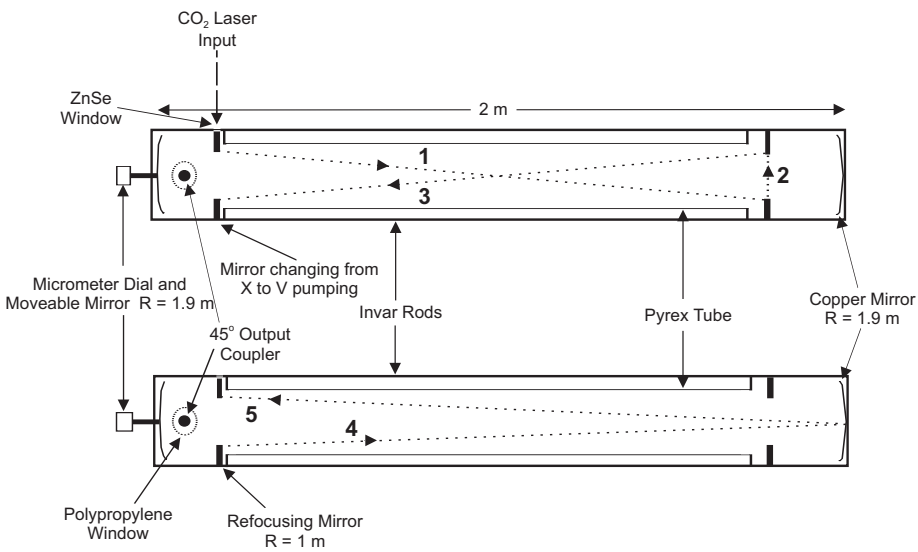

Figure 2. Side view of the FIR laser cavity

[1] The 118.8 μm line of CH_3OH is the strongest known optically pumped FIR laser emission.

In the pumping geometry shown in Fig. 2, a 45º mirror first reflects the beam across the vertical plane of the cavity (path 1). At the other end, two identical 45º mirrors are used to redirect the CO_2 beam to the bottom of the input chamber (paths 2 and 3 which complete the X-portion of the pumping scheme). A gold-plated copper mirror with a 1 m radius-of-curvature then reflects the CO_2 beam to the main FIR cavity mirror (path 4). This curvature was chosen so that the beam diameter would be slightly larger than a 40 µm Gaussian beam waist. This optimizes the overlap between the CO_2 laser beam and the short wavelength FIR emissions. Finally the CO_2 beam is reflected from the FIR mirror, to the input 45º mirror, and out of the FIR system (path 5 which completes the V-portion of the pumping scheme). One advantage to this type of pumping design over simpler configurations, such as the V-pumping geometry, is that the additional passes allow more of the gain medium to be pumped.

The FIR cavity is about 2 m long and utilizes a nearly confocal mirror system, consisting of two 1.9 m radius-of-curvature concave gold-coated copper mirrors with a 50 mm diameter. Four invar rods connect the endplates holding the FIR mirrors and the 2 m long Pyrex glass tube with a 59 mm inner diameter. One copper mirror is attached to a micrometer and is moved to tune the cavity and couples the FIR power out horizontally through a polypropylene window, 0.635 µm thick. The output coupling is varied by moving the 45º copper mirror radially in and out of the cavity mode. The generated FIR radiation is focused by an off-axis parabolic mirror onto a metal-insulator-metal (MIM) point contact diode.

Preliminary wavelength measurements of the FIR radiation were made by tuning the Fabry-Perot cavity with the moveable end mirror and measuring the mirror displacement for 10 wavelengths of that laser mode. The value obtained is accurate to within ± 0.5 µm. A set of absorbing filters calibrated with wavelength attenuates the CO_2 laser radiation and helps distinguish different FIR wavelengths. The relative polarizations of the FIR emissions with respect to the CO_2 laser lines were measured with a multi-Brewster-angle polarization selector.

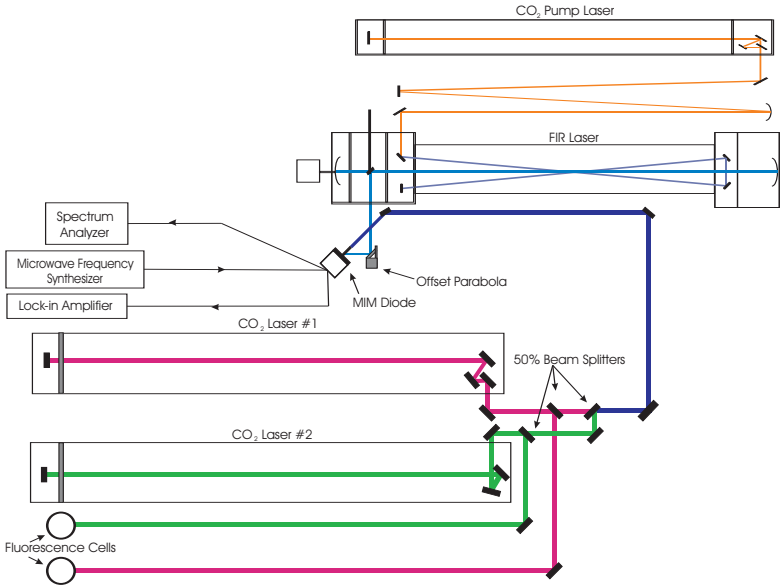

Figure 3. The three-laser heterodyne frequency measurement system

The frequencies of optically pumped FIR laser lines were accurately measured using the three-laser heterodyne technique discussed in detail in Refs. 20 and 21 and illustrated in Figure 3. In general, different but known frequencies are mixed together to produce a sum or difference frequency. This frequency is then combined with a signal of unknown frequency. A "beat"[2] between the unknown and the sum or difference frequency can then be observed on a spectrum analyzer. If the separation between these frequencies is greater than the range of the spectrum analyzer, a microwave source may be added to decrease the gap.

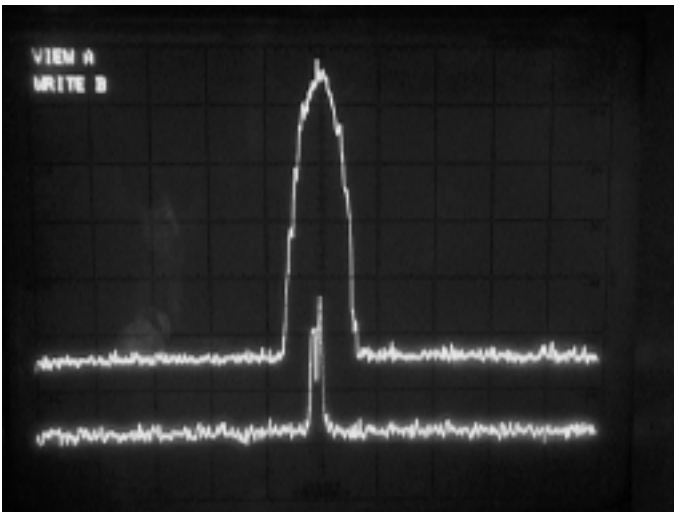

Figure 4. Spectrum analyzer display of the time-averaged beat note between the difference frequency (generated by the 9*R*18 and 10*R*30 CO_2 laser lines), the microwave source, and the unknown FIR frequency for optically pumped CD_3OH. The center frequency is 2850703.9 MHz.

In our experimental system, two CO_2 laser frequencies were combined to create a difference frequency in the FIR region. The particular lines chosen to generate the difference frequency were based on the wavelength measurement of the unknown FIR emission. These CO_2 frequencies were stabilized by locking each laser to a saturation dip in the 4.3 μm fluorescence signal from an external reference cell. The beat note, monitored by means of a spectrum analyzer and shown in Fig. 4, is used to determine the unknown frequency ν_{FIR} through the relation:

$$\nu_{FIR} = \left| n_1\nu_{CO2}(I) - n_2\nu_{CO2}(II) \right| \pm m\nu_{\mu wave} \pm \nu_{beat} \qquad (1)$$

where n_1, n_2 and m are integers that correspond to the respective harmonics (first-order, second-order, etc.) generated in the MIM diode and ν_{beat} is the beat frequency. A MIM point contact diode was used as a harmonic mixer, combining the signals from the laser and microwave sources. The signal from the MIM diode was fed into a preamplifier connected to a HP8355A spectrum analyzer to measure the intermediate frequency beat note by comparison with a marker generated by an Adret CS202 synthesizer. When necessary, a microwave source, HP8350B sweeper, operating between 0 and 18 GHz was used. The frequency of the microwave radiation from the sweeper was measured by means of a HP5343A frequency counter. The values of n_1, n_2, m and the ± sign in Eq. (1) are determined experimentally by

[2] This is analogous to the beat heard between two similar musical tones.

either tuning the FIR laser cavity or by increasing (or decreasing) the microwave frequency slightly in order to get a small shift in the beat note on the spectrum analyzer.

The uncertainty of a frequency measurement is $D\nu/\nu = 2 \times 10^{-7}$ (± 0.2 MHz). It is due mainly to the uncertainty in the setting of the FIR laser cavity to the center of its gain curve. For minimizing this uncertainty, we tuned the FIR laser across its gain curve and observed the change to the beat note on the spectrum analyzer using a peak hold feature. The value of this frequency is calculated from the average of ten measurements recorded with varying microwave frequencies. In addition, these measurements were made with at least two different sets of CO_2 laser lines.

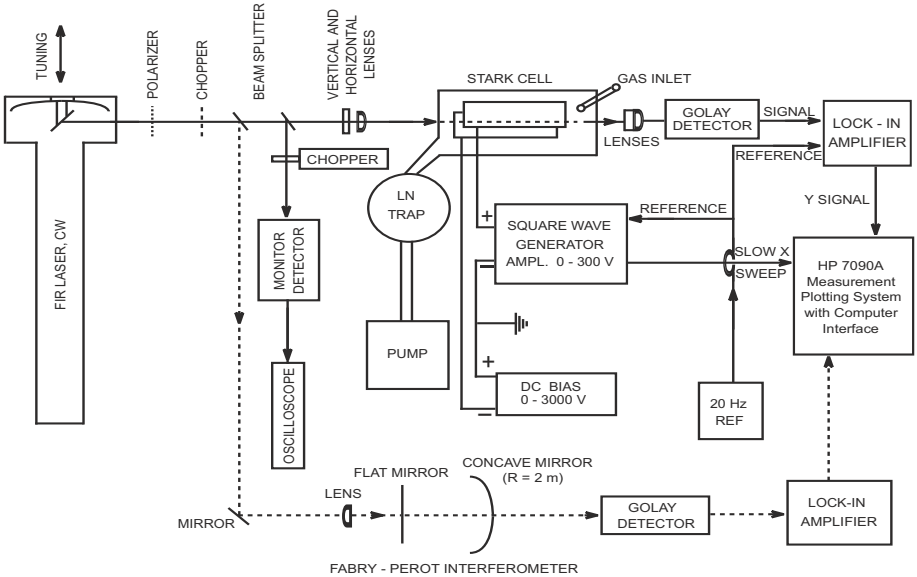

Figure 5. The laser Stark spectroscopy system

Laser Stark spectroscopy of the methanol isotope CD_3OD was investigated using the DCN laser and Stark spectrometer [22]. A block diagram of this experimental system is shown in Fig. 5. The FIR laser is a continuous wave (CW) direct discharge molecular gas laser operating with deuterium cyanide (DCN) at a pressure of 2 Torr. A 5000 W power supply provides the electrical discharge required for lasing to occur with approximately 2000 V dropped across the laser while the other 3000 V are dropped across a ballast. The ballast is required to maintain a constant current through the entire FIR laser system and consists of fifty-six 200 W light bulbs connected in series. This FIR laser has a semi-confocal mirror arrangement with a mirror-to-mirror spacing of 3.8 m. The FIR radiation is coupled out of the laser cavity by 45º diagonal brass mirror, with a 0.64 cm diameter, and through a mylar window. A 1000 lines/inch gold wire-grid polarizer is used to polarize the laser beam either parallel or perpendicular to the Stark electric field. The beam is focused through the Stark cell by a combination (cylindrical-spherical) polyethylene lens that provides the horizontal and vertical steering. The Stark cell is composed of two parallel, silvered glass plates separated by eight quartz spacers with a 0.051 508 ± 0.000 050 cm thickness [23]. During data acquisition, a

continuous flow of molecular sample is maintained through the Stark cell and liquid nitrogen trap, connected to a vacuum pump. A second cylindrical-spherical combination polyethylene lens is placed at the end of the Stark cell to focus the beam into the main Golay detector. The detector transforms the laser radiation into electric pulses processed by a lock-in amplifier and sent to an x-y recorder. The molecular absorption is modulated by a 20 Hz variable amplitude square wave voltage applied to the top plate of the Stark cell. For typical scans, the amplitude of the modulated voltage goes from 0 to 300 V and serves as the x-input of the recorder. A regulated DC power supply provides a negative voltage bias, up to -3000 V, to the lower Stark plate. Thus the effective Stark voltage is the algebraic difference of voltages on the two Stark plates, i.e., the positive voltage of the square wave on the top plate and the negative bias voltage on the lower plate. Uniform electric fields up to 60 000 V/cm can be produced between the Stark plates. By varying the Stark voltage, various resonance peaks are swept through the fixed laser frequency producing the Stark spectra. In order to reduce the effect of mechanical and building vibration, the entire experimental system is anchored on a rigid 1 Ton steel table; and the table is vibration-isolated by suspending it from three vertical nylon ropes each 12 feet long.

RESULTS

Table 1 presents the wavelength listing of the FIR laser emissions discovered in this investigation. The polarization relative to the pump laser, operating pressure and relative intensity are listed. The intensity of the FIR output is given as a listing ranging from Very Very Strong (VVS) to Very Weak (VW). In this work, a VVS line is expected to provide a power greater than 10 mW when all the parameters (pump laser, FIR resonantor, coupling mirror, pressure, etc.) have been optimized. Optimization of the FIR cavity was done to the best of our ability, but in no way should be taken as an absolute measure since the relative intensities of FIR emissions is subject to the experimental apparatus used [24]. The lines labeled with VS, S, M, W and VW have ranges in power from 10-1 mW, 1-0.1 mW, 0.1-0.01 mW, 0.01-0.001 μW and below 1 mW, respectively.

Table 2 gives the frequency measurements of the OPML emissions. All frequency measurements are new and are arranged in order by their pump lines. The wavelengths and wavenumbers were calculated from the average frequency using 1 cm^{-1} = 29 979.2458 MHz. With the CD_3OH laser emission from the 10*R*32 pump line, two peaks were observed. These peaks, separated by approximately 5.3 MHz, may indicate a doublet or an experimental artifact based on the laser cavity used. This includes, but is not limited to, the possibility of observing a higher order TEM mode, or by pumping the FIR medium on the edge rather than in the center of its gain curve. Determining its spectroscopic assignment can only prove the existence of a doublet. Experimental verification could be found by observing this line in another type of FIR cavity. The FIR frequencies were measured for the first time in this work under optimal operating conditions. A slight shift in frequency (possibly a few MHz) may still occur due to the type of FIR cavity and pumping geometry used [24-26].

With the new FIR laser spectroscopic data presented in Table 2 for $^{13}CH_3OH$, it was possible to confirm the assignment for two laser schemes. The first involves the FIR laser transitions $(2, 1^+; 11)^{co} \rightarrow (2, 0; 12)^{co}$ *A* and $(2, 1^+; 11)^{co} \rightarrow (2, 0; 10)^{co}A$ belonging to $^{13}CH_3OH$ and pumped by the 9*P*32 CO_2 line. This CO_2 line was found to be in agreement with the IR absorption transition $(2, 1^+; 10)^0 \rightarrow (2, 1^+; 11)^{co}$ *A*. The customary $(n, K; J)^v$ σ energy-level notation [4, 29, 47, 48], in which n is the quantum number associated to the torsional state, J is the total angular momentum and K is its projection along the internal rotation axis is used

Table 1. New laser emissions from optically pumped methanol isotopes

Pump	Wavelength (μm)	Relative Polarization	Pressure (mTorr)	Relative Intensity
$^{13}CH_3OH$				
9*P*16	75.002[a]	∥	85	S
$^{13}CD_3OD$				
9*R*30	68.837[a]	∥	170	M
9*R*30	103.050[a]	⊥	130	M
9*R*20	111.653[a]	⊥	160	M
9*R*20	135.243[a]	∥	160	M
9*R*8	122.233[a]	∥	115	M
9*P*14	109.996[a]	∥	150	S
9*P*32	100.430[a]	∥	140	M
9*P*44	114.6[b]	⊥	90	W
10*R*40	91.3[b]	⊥	140	M
10*R*40	103.0[b]	∥	170	M
10*R*30	76.4[b]	⊥	250	M
10*R*24	81.8[b]	∥	250	M
10*R*20	65.716[a]	⊥	150	M
10*R*18	109.0[b]	⊥	160	W
10*R*16	57.5[b]	∥	160	M
10*R*16	105.492[a]	⊥	165	M
CHD_2OH				
9*P*18	180.102[a]	∥	110	W

[a] Wavelength derived from frequency measurement presented in Table 2.
[b] Wavelength uncertainty is ± 0.5 μm.

Table 2. New frequency measured laser emissions from optically pumped methanol isotopes

Pump	Wavelength (μm)	Frequency (MHz)	Wavenumber (cm^{-1})	Reference
$^{13}CH_3OH$				
9*P*16	54.087	5 542 754.1	184.8864	27
9*P*16	75.002	3 997 130.4	133.3299	new
9*P*32	71.233	4 208 625.8	140.3846	28
9*P*32	95.459	3 140 541.4	104.7572	28
9*P*32	142.280	2 107 052.9	70.2837	29
9*P*44	124.235	2 413 101.5	80.4924	30
9*P*46	120.144	2 495 277.3	83.2335	30
10*R*40	106.679	2 810 226.5	93.7391	27
10*R*38	97.682	3 069 068.0	102.3731	30
10*R*14	64.589	4 641 523.8	154.8246	29
10*R*14	86.171	3 479 033.7	116.0481	30
CD_3OH				
9*R*6	67.930	4 413 279.2	147.2111	31
10*R*36	68.117	4 401 126.5	146.8058	32
10*R*34	44.256	6 774 066.2	225.9585	31, 33
10*R*32	83.680	3 582 585.2	119.5022	32, 34-36
10*R*32	83.681	3 582 579.9	119.5020	32, 34-36
10*R*16	86.565	3 463 216.2	115.5205	37, 38
10*P*32	105.164	2 850 703.9	95.0892	39
CD_3OD				
9*R*38	64.395	4 655 489.8	155.2904	40, 41
9*P*16	131.185	2 285 263.2	76.2282	41
9*P*26	139.553	2 148 234.9	71.6574	42
9*P*28	63.692	4 706 877.3	157.0045	41
10*R*10	85.450	3 508 415.9	117.0282	40
10*P*10	151.092	1 984 174.4	66.1849	41, 42
$^{13}CD_3OD$				
9*R*30	68.837	4 355 080.6	145.2699	new
9*R*30	103.050	2 909 204.6	97.0406	new
9*R*20	111.653	2 685 044.8	89.5635	new
9*R*20	135.243	2 216 701.1	73.9412	new
9*R*8	122.233	2 452 635.3	81.8111	new
9*P*14	109.996	2 725 481.8	90.9122	new
9*P*24	150.896	1 986 747.5	66.2708	43
9*P*28	151.832	1 974 500.7	65.8623	43
9*P*32	100.430	2 985 091.5	99.5719	new
10*R*20	65.716	4 561 935.4	152.1698	new
10*R*20	70.467	4 254 362.4	141.9103	44
10*R*16	105.492	2 841 850.2	94.7939	new
CHD_2OH				
9*R*30	120.895	2 479 771.1	82.7163	45
9*R*30	134.424	2 230 205.7	74.3917	45
9*P*18	180.102	1 664 566.7	55.5240	new
10*R*18	127.386	2 353 414.0	78.5014	45
10*P*16	102.906	2 913 263.4	97.1760	45
10*P*18	212.406	1 411 410.8	47.0796	45
10*P*18	238.040	1 259 422.3	42.0098	46

here. The quantum number ν labels the vibrational state as ν = 0 for the ground state and ν = co for the excited CO-stretch state. The label σ stands for the symmetry species, *A* or *E*, common to the upper and lower level of the transition. Figure 6 shows the energy level and transition diagram for the 9*P*32 system. The dashed lines represent the IR (capital letter) and FIR (small letter) absorption transitions observed in the Fourier transform spectrum and assigned by the Ritz program [49]. The bold dashed transition (P) is in good coincidence with 9*P*32 CO_2 laser. The observed 95.459 and 71.233 μm laser lines, listed in Table 2, are denoted as L_b and L_c, respectively. L_a (17.0087 cm^{-1}) is one further transition that may potentially yield FIR laser emissions. The wavenumbers of the L_b and L_c laser transitions can be determined, for instance, as follows:

$$L_b = d + E - B = 104.7565\ cm^{-1} \text{ and } L_c = a + \mathbf{P} - F = 140.3843\ cm^{-1}.$$

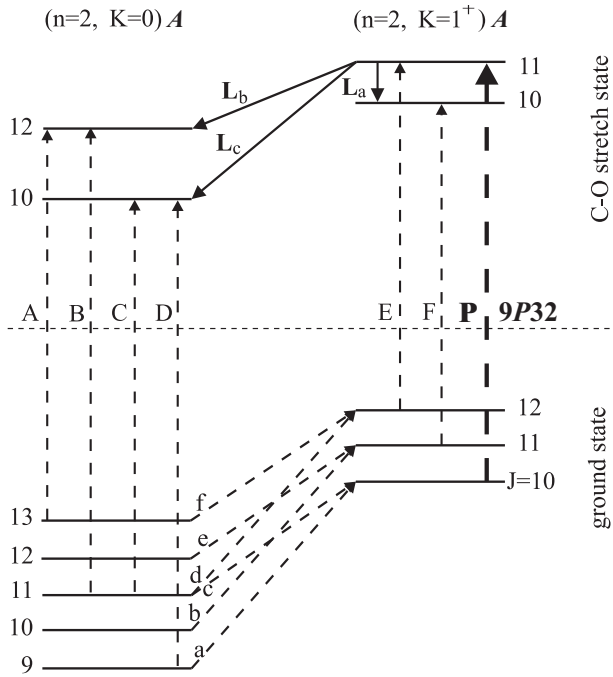

Figure 6. Laser scheme pumped by the CO_2 pump line 9*P*32. The experimental FIR laser wavenumbers are L_b = 104.7572 and L_c = 140.3846 cm^{-1}. The IR (capital letter) and FIR (small letter) FT absorption transition wavenumbers (in cm^{-1}) are: A = 995.4067, B = 1034.6032, C = 998.9750, D = 1031.9054, E = 999.4779, F = 1001.2474, P = 1035.4706, a = 136.8191, b = 138.3522, c = 103.8887, d = 139.8818, e = 102.2885 and f = 100.6860

Independent combination loops automatically formed by the Ritz program lead to the average values of 104.7572 and 140.3846 cm^{-1}, which are in agreement with the frequencies measured. Furthermore, the new polarization measurement for the 104.7572 cm^{-1} emission confirms its initial observation [29], reinforcing the previous proposed assignment.

The second assigned system, proposed by Moraes and co-workers [29], involves the 10*R*14 CO_2 line and is shown in Figure 7. In this system, the pump transition is between the $(1, 4; 25)^0$

and (1, 4; 24)^{co} energy levels, both belonging to *E* symmetry. The proposed assignment for the known 269.9 μm (37.05 cm^{-1}) FIR laser line led to the prediction of the 86.5 μm (115.87 cm^{-1}) line. The recent observation of this laser emission [30] has led to its frequency measurement. The wavenumbers calculated by the Ritz program for these three FIR lines pumped by 10*R*14 CO_2 line were 37.1214 (L_a in Fig. 7), 116.0482 (L_b) and 154.8247 cm^{-1} (L_c). The frequency measurements presented here for the L_b and L_c lines are in exact agreement with the values derived, confirming the assignment for this laser scheme.

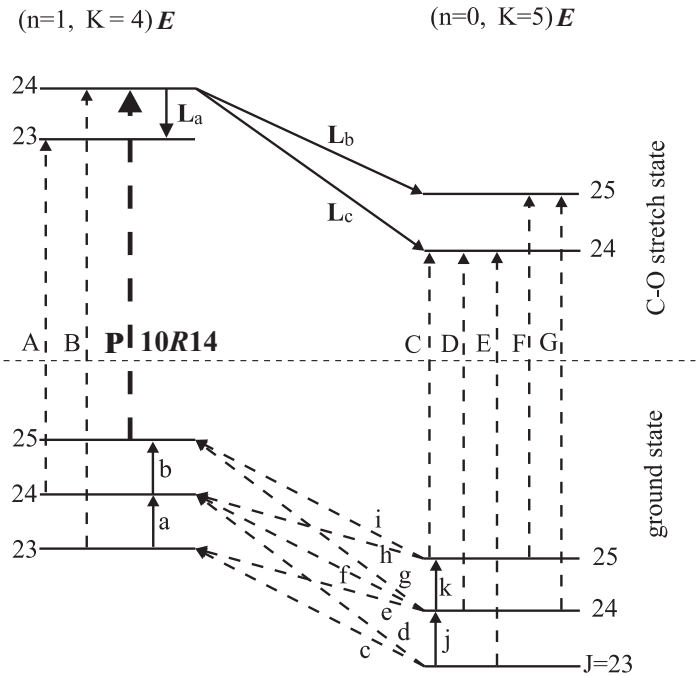

Figure 7. Laser scheme pumped by the CO_2 pump line 10*R*14. The experimental FIR laser wavenumbers are L_a = 37.05, L_b = 116.0481 and L_c = 154.8246 cm^{-1}. The IR (capital letter) and FIR (small letter) FT absorption transition wavenumbers (in cm^{-1}) are: A = 973.9444, B = 1048.6439, C = 973.5891, D = 1012.8362, E = 1050.5231, F = 1012.3657, G = 1051.6132, P = 971.9312, a = 37.5780, b = 39.1350, c = 156.7040, d = 194.2821, e = 119.0176, f = 156.5958, g = 195.7302, h = 117.3480, i = 156.4825, j = 37.6860 and k = 39.2477.

The Stark spectra for CD_3OD were recorded using the 195 μm line of the DCN laser. The spectra were taken in both parallel and perpendicular polarizations up to 60 000 V/cm. Several families of resonances have been observed for CD_3OD with the 195 μm DCN laser line. Figure 8 shows the spectrum in the perpendicular polarization ($\Delta M = \pm 1$) in the low voltage region. From the variation in the relative intensity of the absorption peaks, it was determined that the peaks belonged to a P- or R-branch transition using the method of analysis described in Ref. 22. The maximum M value for this transition observed in the $\Delta M = 0$ spectra was assigned to be 15. With the detuning experiment [22], it was determined that the zero-field frequency of this transition lies above the 195 μm laser line in energy. From the

energy level predictions based on the reported molecular constants [50], the transition was tentatively assigned to the P-branch transition $J_K = 15_2 \leftarrow 16_3\ A^-$, $\upsilon_t = 2$. This is the first time this transition has been observed experimentally by any technique.

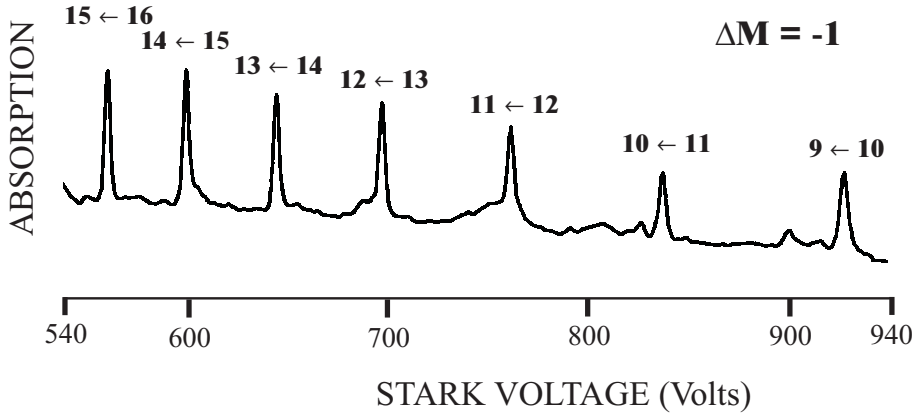

Figure 8. Stark absorption spectra from 540 to 940 V for the $J_K = 15_2 \leftarrow 16_3\ A^-$, $\upsilon_t = 2$ transition of CD_3OD in the perpendicular polarization recorded with the 195 μm line of the DCN laser. The Stark cell pressure was 35 mTorr

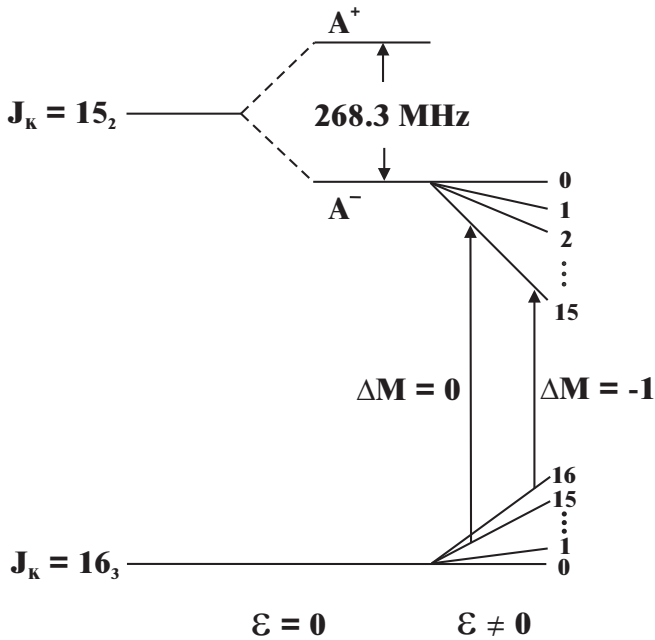

Figure 9. Energy level structure, estimated K-doubling and schematic Stark effects for the $J_K = 15_2 \leftarrow 16_3\ A^-$, $\upsilon_t = 2$ transition of CD_3OD. Typical M components are shown of the $\Delta M = 0$ and $\Delta M = -1$ classes observable at the fixed-laser frequency as the Stark field ε is increased

The Stark coefficients for the K = 2*A* and K = 3*A* levels were calculated by our collaborators using the available molecular parameters and the method described by Johnston et al. [22]. For the J = 15, K = 2*A* level, the asymmetry splitting is comparable to the Stark shift so one needs the exact diagonalization method involving the –K and +K mixed states. Figure 9 illustrates the energy levels involved in the A^- transition. The first- and second-order Stark shift for the 15_2 level is calculated using the relation

$$\Delta\nu = -\{(\Delta^2/4 + C^2M^2\varepsilon^2)^{1/2} - \Delta/2\} + (A + BM^2)\varepsilon^2 \quad (2)$$

where A, B and C are the Stark coefficients for a particular level, M is the fixed component of the angular momentum J along the direction of the electric field ε and Δ is the splitting of the K = 2*A* level. For 16_3, the asymmetry splitting is negligible and therefore the first- and second order Stark shifts are calculated using the relation

$$\Delta\nu = -CM\varepsilon + (A + BM^2)\varepsilon^2 \quad (3)$$

The calculated net Stark shifts for peaks observed in the parallel and perpendicular polarization are presented in Table 3. A negative sign in the net Stark shift corresponds to a transition frequency above the laser frequency. The zero-field transition frequency ν_{tr} is calculated by subtracting the net Stark shift from the laser frequency ν_L, i.e.,

$$\Delta\nu = \nu_L - \nu_{tr}. \quad (4)$$

For ν_L, a value of 1 539 745.0 ± 3.1 MHz was used for the 195 μm line [51]. The average of the net Stark shifts in Table 3 for this transition is –547.8 ± 6.7 MHz, where we simply take the root-mean-square deviation of the shifts as the measure of the error. The average net shift gives an experimental zero-field frequency of 1 540 292.8 ± 7.4 MHz.

Table 3. Observed Stark voltages and calculated Stark shifts (in MHz) for the $J_K = 15_2 \leftarrow 16_3$ A^-, υ_t = 2 of CD_3OD in the parallel and perpendicular polarization at λ = 195 μm

M′	←	M″	Stark Voltage (Volts)	First Order Stark Shift	Second Order Stark Shift	Net Stark Shift
15	←	15	574.0	-508.47	-47.75	-556.22
14	←	14	616.5	-509.96	-46.44	-556.40
13	←	13	666.0	-511.88	-44.81	-556.69
12	←	12	722.0	-512.31	-42.45	-554.76
11	←	11	790.0	-514.16	-39.58	-553.74
10	←	10	872.0	-516.29	-35.71	-552.00
9	←	9	975.0	-520.20	-30.48	-550.68
8	←	8	1104.0	-524.25	-22.85	-547.10
7	←	7	1280.0	-533.36	-11.45	-544.81
15	←	16	558.0	-495.34	-52.57	-547.91
14	←	15	598.0	-495.76	-51.69	-547.45
13	←	14	643.0	-495.15	-50.38	-545.53
12	←	13	696.0	-495.02	-48.79	-543.81
11	←	12	761.0	-496.83	-47.00	-543.83
10	←	11	837.0	-497.29	-44.24	-541.53
9	←	10	928.0	-496.65	-40.23	-536.88
8	←	9	1047.0	-499.18	-34.92	-534.10

CONCLUSIONS

We report the discovery of eighteen new OPML emissions, forty-three frequency measurements of optically pumped methanol isotopes, the assignments of two laser schemes for $^{13}CH_3OH$ and the assignment of the CD_3OD absorption transition $J_K = 15_2 \leftarrow 16_3\ A^-$, $\upsilon_t = 2$. The new OPML emissions will be useful for filling the gaps currently existing in this short-wavelength portion of the FIR region. Due to the accuracy with which the laser frequencies were measured, this work will be useful for future assignments of FIR laser emissions from these molecules by calculation of combination loops from high-resolution Fourier transform data [52-54]. These results can also be used for Stark spectroscopy and laser magnetic resonance where OPML emissions serve as a source of strong coherent FIR radiation. Despite the uncertainties in the Stark effect, the FIR transition frequency measured here represents an increase in accuracy over the calculated frequencies for CD_3OD. Finally, the information gained from these frequencies will help provide a more complete picture of these molecules in the far-infrared region.

ACKNOWLEDGEMENTS

The authors are pleased to acknowledge the following programs for financial support: the National Science Foundation (CRIF - #9982001 and RUI - #0078812), the Wisconsin Space Grant Consortium (Faculty Research Seed Grant and Undergraduate Research Award), Sigma Xi (Grants-in-Aid of Research), the College of Science and Allied Health (Faculty Research Grant and Undergraduate Research Grant), and the University of Wisconsin–La Crosse (Undergraduate Research Grant). We would also like to acknowledge our collaborators for their contributions to this work: Dr. K. M. Evenson, Dr. M. D. Allen, Dr. E. C. C. Vasconcellos, Dr. J. C. S. Moraes, Dr. R. M. Lees, Dr. Li-Hong Xu and Dr. I. Mukhopadhyay.

REFERENCES

1. A. Borden and E. F. Barker, “The Infra-Red Absorption Spectrum of Methyl Alcohol”, *J. Chem. Phys.*, **6**, 553-563 (1939).
2. J. S. Koehler and D. M. Dennison, “Hindered Rotation in Methyl Alcohol”, *Phys. Rev.*, **57**, 1006-1021 (1940).
3. Li-Hong Xu and J. T. Hougen, “Global Fit of Rotational Transitions in the Ground Torsional State of Methanol”, *J. Mol. Spectrosc.*, **169**, 396-409 (1995).
4. G. Moruzzi, B. P. Winnewisser, M. Winnewisser, I. Mukhopadhyay, and F. Strumia, “Microwave, Infrared and Laser Transitions of Methanol: Atlas of Assigned Lines from 0 to 1258 cm^{-1}”, CRC Press, Boca Raton (1995).
5. J. A. Ball, C. A. Gottlieb, A. E. Lilley, and H. E. Radford, “Detection of Methyl Alcohol in Sagittarius”, *Astrophys. J. Letts.*, **168**, L203-L210 (1970).
6. M. F. Chui, A. C. Cheung, D. Matsakis, C. H. Townes, and A. G. Cardiasmenos, “Methanol Source in Orion at 1.2 Centimeters”, *Astrophys. J.*, **187**, L19-L21 (1974).
7. R. Hills, V. Pankonin, and T. L. Landecker, “Evidence for Maser Action in 1.2 cm Transitions of Methanol in Orion”, *Astr. Astrophys.*, **39**, 149-153 (1975).
8. T. Anderson, E. Herbst, and F. C. Delucia, “An Extension of the High-Resolution Millimeter- and Submillimeter-Wave Spectrum of Methanol to High Angular Momentum Quantum Numbers”, *Astrophys. J. Suppl.*, **82**, 405-444 (1992).

9. T. Anderson, E. Herbst, and F. C. Delucia, "The Millimeter- and Submillimeter-Wave Spectrum of $^{13}CH_3OH$ Revisited", *Astrophys. J. Suppl.*, **74**, 647-664 (1990).
10. T. Anderson, R. L. Crownover, E. Herbst, and F. C. Delucia, "The Laboratory Millimeter- and Submillimeter-Wave Spectrum of CH_3OD", *Astrophys. J. Suppl.*, **67**, 135-148 (1988).
11. D. Pereira, J. C. S. Moraes, E. M. Telles, A. Scalabrin, F. Strumia, A. Moretti, G. Carelli, and C. A. Massa, "A Review of Optically Pumped Far-Infrared Laser Lines From Methanol Isotopes", *Int. J. Infrared and Millimeter Waves*, **15**, 1-44 (1994).
12. E. C. C. Vasconcellos and S. C. Zerbetto, "Far Infrared Laser Lines Produced by Methanol and its Isotopic Species: A Review", *Int. J. Infrared and Millimeter Waves*, **15**, 889-899 (1994).
13. N. G. Douglas, "Millimeter and Submillimeter Wavelength Lasers: A Handbook of CW Measurements", Springer-Verlag, New York (1989).
14. S. Jacobsson, "Review – Optically Pumped Far Infrared Lasers", *Infrared Phys.*, **29**, 853-874 (1989).
15. E. C. C. Vasconcellos, S. C. Zerbetto, J. C. Holecek, and K. M. Evenson, "Short-Wavelength Far-Infrared Laser Cavity Yielding New Lines in Methanol", *Opt. Letts.*, **20**, 1392-1393 (1995).
16. E. M. Telles, H. Odashima, L. R. Zink, and K. M. Evenson, "Optically Pumped FIR Laser Lines from CH_3OH: New Laser Lines, Frequency Measurements, and Assignments", *J. Mol. Spectrosc.*, **195**, 360-366 (1999).
17. C-C. Chou, K. M. Evenson, L. R. Zink, A. G. Maki, and J-T Shy, "New CO_2 Laser Lines in the 11-µm Wavelength Region: New Hot Bands", *IEEE J. Quantum Electron.*, **QE-31**, 343-345 (1995).
18. K. M. Evenson, C-C. Chou, B. W. Bach, and K. G. Bach, "New CW CO_2 Laser Lines: The 9-µm Hot Band", *IEEE J. Quantum Electron.*, **QE-30**, 1187-1188 (1994).
19. M. Jackson, E. M. Telles, M. D. Allen, and K. M. Evenson, "Short-Wavelength Far-Infrared Laser Cavity Yielding New Laser Emissions in CD_3OH", *Appl. Phys. B* **72**, 815-818 (2001).
20. F. R. Petersen, K. M. Evenson, D. A. Jennings, J. S. Wells, K. Goto, and J. J. Jimenez, "Far Infrared Frequency Synthesis with Stabilized CO_2 Lasers: Accurate Measurements of the Water Vapor and Methyl Alcohol Laser Frequencies", *IEEE J. Quantum Electron.*, **QE-11**, 838-843 (1975).
21. For example: Li-Hong Xu, R. M. Lees, E. C. C. Vasconcellos, S. C. Zerbetto, L. R. Zink, and K. M. Evenson, "Methanol and the Optically Pumped Far-Infrared Laser", *IEEE J. Quantum Electron.*, **QE-32**, 392-398 (1996).
22. L. H. Johnston, R. P. Srivastava, and R. M. Lees, "Laser Stark Spectrum of Methyl Alcohol at 890.761 GHz with the HCN Laser", *J. Mol. Spectrosc.*, **84**, 1-40 (1980).
23. L. H. Johnston, S. R. Raju, and G. R. Sudhakaran, "Methanol Lines for Stark Cell Calibration", *J. Mol. Spectrosc.*, **89**, 556 (1981).
24. D. T. Hodges, "A Review of Advances in Optically Pumped Far-Infrared Lasers", *Infrared Phys.*, **18**, 375-384 (1978).
25. E. M. Telles, L. R. Zink, and K. M. Evenson, "Frequencies of Optically Pumped Sub-Doppler Far-Infrared Laser Lines of Methanol", *J. Mol. Spectrosc.*, **191**, 206-208 (1998).
26. M. Inguscio, L. R. Zink, K, M. Evenson, and D. A. Jennings, "Accurate Frequency of the 119 µm Methanol Laser from Tunable Far-Infrared Absorption Spectroscopy", *IEEE J. Quantum Electron.*, **QE-26**, 575-579 (1990).

27. J. C. S. Moraes, A. Bertolini, G. Carelli, N. Ioli, A. Moretti, and F. Strumia, "The $^{13}CH_3OH$ Optically Pumped Far-Infrared Laser: New Lines and Frequency Measurements", *IEEE J. Quantum Electron.*, **32**, 1737-1739 (1996).
28. N. Ioli, A. Moretti, F. Strumia, and F. D'Amato, "$^{13}CH_3OH$ and $^{13}CD_3OH$ Optically Pumped FIR Laser: New Large Offset Emission and Optoacoustic Spectroscopy", *Int. J. Infrared and Millimeter Waves*, **7**, 459-485 (1986).
29. J. C. S. Moraes, G. Carelli, A. Moretti, G. Moruzzi, and F. Strumia, "Assignments of FIR laser lines from optically pumped $^{13}CH_3OH$", *J. Mol. Spectrosc.*, **177**, 302-306 (1996).
30. J. C. S. Moraes, O. P. Pizoletto, A. Scalabrin, M. D. Allen, and K.M. Evenson, "Investigation of $^{13}CH_3OH$ methanol: new laser lines and assignments", *Appl. Phys. B*, **72**, 241-244 (2001).
31. G. Carelli, N. Ioli, A. Moretti, D. Pereira, and F. Strumia, "New Large Offset Far-Infrared Laser Lines from CD_3OH", *Appl. Phys. B*, **44**, 111-117 (1987).
32. S. Haunt, M. A. Hopkins, K. Karrai, G. Dampne, R. J. Nicholas, L. C. Brunel, "New Wavelength Measurements and Laser Lines in Optically Pumped Methanol and Methanol Analogues", *Revue Phys. Appl.*, **22**, 205-206 (1987).
33. H. Sigg, H. J. A. Bluyssen, and P. Wyder, "New Laser Lines with Wavelengths from λ = 61.7 μm Down to λ = 27.7 μm in Optically Pumped CH_3OH and CD_3OH", *IEEE J. Quantum Electron.*, **QE-20**, 616-617 (1984).
34. T. Yoshida, T. Yoshihara, K. Sakai, and S. Fujita, "The Stark Effect on Optically Pumped CH_3OD and CD_3OH Lasers", *Infrared Phys.*, **22**, 293-298 (1982).
35. D. Pereira, C. A. Ferrari, and A. Scalabrin, "New Optically Pumped FIR Laser Lines in CD_3OH", *Int. J. Infrared and Millimeter Waves*, **7**, 1241-1250 (1986).
36. G. Carelli, N. Ioli, A. Moretti, D. Pereira, and F. Strumia, "Measurements and Assignments of New Large Offset CD_3OH FIR Laser Lines", *Int. J. Infrared and Millimeter Waves*, **12**, 557-571 (1991).
37. E. J. Danielewicz and C. O. Weiss, "New CW Far-Infrared Laser Lines From CO_2 Laser-Pumped CD_3OH", *IEEE J. Quantum Electron.*, **QE-14**, 458-459 (1978).
38. R. J. Saykally, K. M. Evenson, D. A. Jennings, L. R. Zink, and A. Scalabrin, "New FIR Laser Lines and Frequency Measurements for Optically Pumped CD_3OH", *Int. J. Infrared and Millimeter Waves*, **8**, 653-662 (1987).
39. E. M. Telles, L. R. Zink, and K. M. Evenson, "New FIR Laser Lines from CD_3OH", *Int. J. Infrared and Millimeter Waves*, **19**, 1627-1631 (1998).
40. E. C. C. Vasconcellos, A. Scalabrin, F. R. Petersen, and K. M. Evenson, "New FIR Laser Lines and Frequency Measurements in CD_3OD", *Int. J. Infrared and Millimeter Waves*, **2**, 533-539 (1981).
41. T. Yoshida, M. Kobayashi, T. Yoshihara, K. Sakai, and S. Fujita, "Stark Effect in Submillimeter Laser Lines from Optically Pumped CH_3OH and CD_3OD", *Opt. Commun.*, **40**, 45-48 (1981).
42. D. Pereira, E. C. C. Vasconcellos, A. Scalabrin, K. M. Evenson, F. R. Petersen, and D. A. Jennings, "Measurements of New FIR Laser Lines in CD_3OD", *Int. J. Infrared and Millimeter Waves*, **6**, 877-882 (1985).
43. E. C. C. Vasconcellos and K. M. Evenson, "New Far Infrared Laser Lines Obtained by Optically Pumping $^{13}CD_3OD$", *Int. J. Infrared and Millimeter Waves*, **6**, 1157-1167 (1985).
44. K. M. Evenson, *Private Communication*.

45. J. A. Facin, D. Pereira, E. C. C. Vasconcellos, A. Scalabrin, and C. A. Ferrari, "New FIR Laser Lines from CHD_2OH Optically Pumped by a cw CO_2 Laser", *Appl. Phys. B*, **48**, 245-248 (1989).
46. G. Ziegler and U. Dürr, "Submillimeter Laser Action of cw Optically Pumped CD_2Cl_2, CH_2DOH, and CHD_2OH", *IEEE J. Quantum Electron.*, **QE-14**, 708 (1978).
47. G. Moruzzi, F. Strumia, P. Carnesecchi, B. Carli, and M. Carlotti, "High Resolution Spectrum of CH_2OH between 8 and 100 cm^{-1}", *Infrared Phys.*, **29**, 47-86 (1989).48.
48. R. M. Lees and J. G. Baker, "Torsion-Vibration-Rotation Interactions in Methanol. I. Millimeter Wave Spectrum", *J. Chem. Phys.*, **48**, 5299-5318 (1968).
49. J. C. S. Moraes, D. Pereira, A. Scalabrin, G. Moruzzi, F. Strumia, B. P. Winnewisser, M. Winnewisser, I Mukhopadhyay and P. K. Gupta, "Ritz Analysis of the Fourier Transform Spectrum of $^{13}CH_3OH$ from 25 to 250 cm^{-1}", *J. Mol. Spectrosc.*, **174**, 177-195 (1995).50.
50. R. M. Lees, *Private Communication*.
51. L. O. Hocker and A. Javan, "Absolute Frequency Measurements of New CW DCN Submillimeter Laser Lines", *Appl. Phys. Lett.*, **12**, 124-125 (1968).
52. R. M. Lees, "Far-infrared laser spectroscopy of Methanol: A Probe for Vibrational Mode Coupling", *Proc. SPIE, Millimeter and Submillimeter Waves II*, M. N. Afsar; Ed., **2558**, 262-284 (1995).
53. J. O. Henningsen, Chapter 2 – "Molecular Spectroscopy by Far-Infrared Laser Emission", *Infrared and Millimeter Waves – Coherent Sources and Applications, Part I*, K. J. Button; Ed., **5**, 29-128 (1982).
54. J. O. Henningsen, "Assignment of Laser Lines in Optically Pumped CH_3OH", *IEEE J. Quantum Electron.*, **QE-13**, 248-252 (1977).